JOURNAL OF COMPUTATIONAL PHYSICS 56, 448–460 (1984)

High-Order Upwind Flux Correction Methods for Hyperbolic Conservation Laws

B. EDWARD MCDONALD AND JOHN AMBROSIANO*

Naval Ocean Research and Development Activity,
Numerical Modeling Division,
NSTL Station, Mississippi 39529

Received May 31, 1983; revised February 21, 1984

Totally one-sided first-order and second-order schemes are presented employing a numerically calculated characteristic speed direction and are combined into a transportive, monotonicity-preserving hybrid scheme using the method of flux correction. The first-order scheme is free of expansion shocks and artificial extrema. The hybrid scheme computes a provisional update from the first-order scheme, and then filters the second-order corrections to prevent occurrence of new extrema. Computed versus analytic results are compared for two different N-wave shocks and for a third case involving linear advection of a square wave. Results are given with and without the second-order correction. The second-order results are always superior to first-order results, with the most dramatic difference occurring in the case of linear advection. The results suggest that higher than second-order upwind differences could be substituted in the hybrid scheme to reduce truncation error even further.

1. INTRODUCTION

The development of flow discontinuities in hyperbolic systems presents substantial difficulties to solution by finite differences. When second-order or higher-order differences are used, the solutions tend to develop dispersive ripples near sharp gradients. When first-order methods are used, the solution suffers from numerical dissipation. In recent years this problem has been addressed by the use of nonlinear filters to control "anti-diffusive" corrections to first-order results (Boris and Book [1], Zalesak [10, 11], Van Leer [7], and Harten [5]). In particular, the method of flux-corrected transport (FCT) [1, 10 11] allows high-order corrections to dominate where the solution is smooth, but retains the low-order solution where the flow is highly structured. The FCT method is capable of producing impressive results for problems involving shock waves and linear advection.

The aim of this paper is to introduce an improvement to the FCT method as applied to scalar hyperbolic conservation laws. Our motivation for developing an improved scheme arose from the need to simulate the formation of shocks from initially smooth profiles. We found that a commonly used FCT scheme employing a

* Permanent address: Berkeley Scholars, Inc., P.O. Box 852, Springfield, Virginia 22150.

0021-9991/84 $3.00

donor cell algorithm as the first part and a flux-limited spatially-centered high-order correction produced some pathological results. The worst of these included the formation of "staircases" on a steepening slope, and in another case a non-physical shock arising out of an expansion region, examples of which are given in the numerical results section. The improvements presented here produced a relatively simple and robust algorithm which is free of these pathologies.

The improvement comes about through the use of totally one-sided differences and a switching of direction based on an estimate of the characteristic speed. One-sided or upwind differences are used both in the low-order monotone step and the high-order correction step. Proponents of upwind differencing have pointed out that such schemes have the advantage of being "transportive"; that is, they convect perturbations of the solution in the direction of the flow. This interpretation has a certain physical appeal (Roach [8]). Spatially high-order upwind differencing does not seem to have found much success on its own, although there have been serious proponents of the approach (Van Leer [7], Warming and Beam [9]). This is probably because of its failure to guarantee monotonicity. Monotonicity is the property of scalar hyperbolic conservation laws which forbids the generation of new extrema or the enhancement of old ones. For example, in an early paper, Van Leer [7] proposed the use of a full second-order upwind scheme to solve Burger's equation. Then noting the monotonicity problem, he proposed using flux-limiting filters to enforce the monotonicity constraint.

In this paper we will demonstrate that the flux-correction technique enables the use of spatially high-order upwind differencing while maintaining the proper monotonicity constraints. We will demonstrate the robustness of the method by solving three test problems: the steepening of an "N-wave" shock (a familiar phenomenon in nonlinear acoustics), both in a fixed and a drifting frame with respect to the center of the disturbance; and the linear advection of a square wave pulse disturbance. Each of these results will be compared with analytic solutions.

We are concerned with hyperbolic systems which can be modeled by the scalar initial value problem

$$\rho_t + \phi(\rho)_x = 0 \tag{1a}$$

$$\rho(x, 0) = \rho_0(x), \tag{1b}$$

where the flux ϕ is a smooth function of ρ. In various applications the dependent variable ρ may play the role of a mass density perturbation or a flow velocity. Thus ρ may be positive or negative in general.

Equation (1a) may be expressed as

$$\rho_t + u(\rho)\rho_x = 0 \tag{2}$$

where

$$u(\rho) = \phi_\rho \tag{3}$$

is known as the characteristic speed. Equation (2) implies the preservation of monotonicity: $\rho_t = 0$ at local extrema.

In some cases Eq. (2) may admit analytic solutions up to the time at which a shock is formed. These solutions may be found by the method of characteristics as follows: Equation (2) demands constancy of ρ along the trajectory

$$x_t = u(\rho). \tag{4}$$

Both x_t and u are constant on this trajectory, so the value of ρ at (x, t) may be found by following the trajectory backward to the initial condition; that is,

$$\rho(x, t) = \rho_0(x - tu(\rho)). \tag{5}$$

Solutions in closed form are generated by solving (5) for ρ in terms of x and t. In the example to be given in Section 3, $u(\rho)$ is taken to be linear and $\rho_0(x)$ quadratic.

If a shock discontinuity in the flow is present, conservation of mass flux across the shock is sufficient to determine the speed at which the shock propagates (i.e., the Rankine–Hugoniot relation). Therefore, a numerical algorithm written in a flux-conservative form should be expected to produce a shock propagating with the correct speed as it emerges from a continuously steepening profile. This will be demonstrated in the results given below.

2. The Hybrid Upwind Method

In this section we present two separate upwind difference schemes and combine them into a hybrid form by the method of flux-correction (Zalesak [10]). For simplicity we assume a constant grid spacing δx. We take ρ_i and ϕ_i to be values at integer grid points, and define half-integer grid variables $f_{i+1/2}$ and $w_{i+1/2}$, where f is a numerical flux to be defined below, and w is a variable which will be used to determine the upwind direction.

A. *The First-Order Scheme*

The numerical method is written as

$$\rho_i^{n+1} = \rho_i^n - f_{i+1/2} + f_{i-1/2} \tag{6}$$

where the superscript gives the timestep number. Quantities lacking a superscript are evaluated at the timestep n. The numerical fluxes are

$$f_{i+1/2} = \begin{cases} \dfrac{\delta t}{\delta x}\phi_i; & w_{i+1/2} \geqslant 0 \\ \dfrac{\delta t}{\delta x}\phi_{i+1}; & w_{i+1/2} < 0. \end{cases} \tag{7}$$

The direction variable w is in principle the characteristic speed. However, we find it more convenient to define w as a quantity with the same sign as the characteristic speed, namely,

$$w_{i+1/2} \equiv (\phi_{i+1} - \phi_i)(\rho_{i+1} - \rho_i). \tag{8}$$

This not only makes the values of w a little faster to compute than a finite difference derivative, but also avoids the risk of division by zero. We may prove that this rather general first-order upwind method possesses the desired monotonicity property by considering the following four possibilities:

Case 1. $w_{i-1/2} \geqslant 0$; $w_{i+1/2} \geqslant 0$.
Equations (6) and (7) give

$$\rho_i^{n+1} - \rho_i^n = -\frac{\delta t}{\delta x}(\phi_i - \phi_{i-1}) \tag{9}$$

or

$$\rho_i^{n+1} - \rho_i^n = -\frac{\delta t}{\delta x}\bar{u}_-(\rho_i - \rho_{i-1}) \tag{10}$$

where

$$\bar{u}_- \equiv (\phi_i - \phi_{i-1})/(\rho_i - \rho_{i-1}) = u(\bar{\rho}_-). \tag{11}$$

This last identity results from the mean value theorem, with $\bar{\rho}_-$ lying in the interval (ρ_{i-1}, ρ_i).
Hence

$$\rho_i^{n+1} = \rho_i(1 - \varepsilon_-) + \rho_{i-1}\varepsilon_- \tag{12}$$

with

$$\varepsilon_- \equiv |\bar{u}_- \delta t/\delta x|. \tag{13}$$

Equation (12) demonstrates that monotonicity is preserved for $\varepsilon_- \leqslant 1$.

Case 2. $w_{i-1/2} < 0$; $w_{i+1/2} < 0$.
For these directions we find

$$\rho_i^{n+1} = \rho_i(1 - \varepsilon_+) + \rho_{i+1}\varepsilon_+ \tag{14}$$

where

$$\varepsilon_+ \equiv |\bar{u}_+ \delta t/\delta x| \tag{15}$$

and

$$\bar{u}_+ = (\phi_{i+1} - \phi_i)/(\rho_{i+1} - \rho_i) = u(\bar{\rho}_+) \tag{16}$$

with $\bar{\rho}_+$ lying in the interval (ρ_i, ρ_{i+1}). For $\varepsilon_+ \leqslant 1$ monotonicity is preserved.

Case 3. $w_{i-1/2} < 0$; $w_{i+1/2} \geqslant 0$.
Equations (6) and (7) yield

$$\rho_i^{n+1} = \rho_i. \tag{17}$$

This reflects that $u = 0$ within one cell of point i and preserves the first-order spatial accuracy of the method. A switching condition *other* than the sign of the characteristic could result in $\rho_j^{n+1} = \rho_j^n$ at a point j more than one cell distant from the point where $\phi_x = 0$. At such a point, even first order accuracy would be lost. An example will be given below in Fig. 2.

Case 3 admits the possibility of stationary *expansion shocks*, if they are present in the initial condition. These nonphysical structures will be defined and dealt with below.

Case 4. $w_{i-1/2} \geqslant 0$; $w_{i+1/2} < 0$.
For this case we have

$$\rho_i^{n+1} - \rho_i^n = -\frac{\delta t}{\delta x}(\phi_{i+1} - \phi_{i-1}). \tag{18}$$

A small amount of algebraic manipulation after adding and subtracting ϕ_i within the parentheses obtains

$$\rho_i^{n+1} = \rho_i(1 - \varepsilon_- - \varepsilon_+) + \rho_{i+1}\varepsilon_+ + \rho_{i-1}\varepsilon_-. \tag{19}$$

This case provides the most stringent condition necessary to guarantee monotonicity (and thus stability as well):

$$|u\delta t/\delta x| \leqslant \tfrac{1}{2}. \tag{20}$$

B. *Expansion Shock Correlation*

Models in which viscosity is unimportant on a macroscopic scale are typically cast as inviscid, and thus remain invariant upon time and velocity reversal. In a physical shock front, however, molecular viscosity transforms kinetic energy to entropy (heat) in an extremely small region of compression. Thus a time-reversed shock (called an expansion shock) is forbidden by the second law of thermodynamics. Physically, this means that a shock discontinuity in an expansion of the flow must cease to be a shock by unsteepening at a rate determined by the expansion. The above scheme admits a steady state solution whenever two distinct values ρ_L and ρ_R exist such that $\phi(\rho_L) = \phi(\rho_R)$. A discontinuous jump from $\rho_L = \text{const}$ to $\rho_R = \text{const}$ will remain stationary by Eq. (1a). When $u(\rho_L) \geqslant 0$ and $u(\rho_R) \leqslant 0$, a compression exists and the shock is valid. To eliminate expansion shocks, however, we assume $u = \partial\phi/\partial\rho$ is known, and replace a single flux in (6) as follows: *Wherever* $u_i < 0$ *and* $u_{i+1} > 0$:

$$f_{i+1/2} \to \frac{1}{2}\left(f_{i+3/2} + f_{i-1/2} - \frac{\delta t}{\delta x}(\rho_{i+1} - \rho_i)(u_{i+1} - u_i)\right). \tag{21}$$

This replacement minimizes with respect to $f_{i+1/2}$ the following measure of discrepancy between finite difference representations of Eqs. (1a) and (2)

$$d \equiv \sum_{j=i}^{i+1} \left(u_j(\rho_{i+1} - \rho_i) \frac{\delta t}{\delta x} - (f_{j+1/2} - f_{j-1/2}) \right)^2. \tag{22}$$

The use of (21) and (6) turns out to be equivalent to the introduction of a shock-local viscosity whose magnitude brings finite difference representations of (1a) and (2) into closest agreement in the least squares sense.

C. *The Higher Order Scheme*

A stable second-order upwind scheme involving the point i and two points to the left or right (depending on the sign of the characteristic) may be defined as follows. A predictor step defines fluxes at time level $n + \frac{1}{2}$ according to the following. Equation (3) gives straightforwardly

$$\phi_t = u\rho_t. \tag{23}$$

We use the first-order fluxes (7) including the expansion correction (21) in

$$\phi_i^{n+1/2} = \phi_i^n - \tfrac{1}{2}u_i(f_{i+1/2} - f_{i-1/2}). \tag{24}$$

Next a corrector step updates ρ using second-order upwind differences on $\phi^{n+1/2}$. One-sided second-order differences may be defined as

$$\frac{\partial \phi}{\partial x}_{x=x_i} \equiv \frac{1}{\delta x}\left[-\frac{3}{2}\phi_i + 2\phi_{i+1} - \frac{1}{2}\phi_{i+2} \right] \tag{25}$$

for differentiation to the right of x_i, and

$$\frac{\partial \phi}{\partial x}_{x=x_i} \equiv \frac{1}{\delta x}\left[\frac{3}{2}\phi_i - 2\phi_{i-1} + \frac{1}{2}\phi_{i-2} \right] \tag{26}$$

for differentiation to the left. We may cast the above in flux conservative form by defining

$$F_{i+1/2} = \frac{\delta t}{\delta x} \cdot \begin{cases} \frac{3}{2}\phi_i^{n+1/2} - \frac{1}{2}\phi_{i-1}^{n+1/2}, & w_{i+1/2} \geqslant 0 \\ \frac{3}{2}\phi_{i+1}^{n+1/2} - \frac{1}{2}\phi_{i+2}^{n+1/2}, & w_{i+1/2} < 0. \end{cases} \tag{27}$$

After F values are computed and stored, the expansion correction (21) is performed with the substitution of F for f. The unfiltered second-order method in flux conservative form would then be

$$\rho_i^{n+1} - \rho_i^n = -F_{i+1/2} + F_{i-1/2}. \tag{28}$$

(Equation (28) appears for the purpose of illustration and is not executed.) The second-order fluxes of (27) will be incorporated into the FCT algorithm which follows. For linear advection at a constant speed the second-order algorithm (24)–(28) is stable for Courant numbers $\varepsilon \leqslant 1$.

D. *The Hybrid Scheme*

We construct the provisional quantities

$$\rho_i^* = \rho_i^n - f_{i+1/2} + f_{i-1/2} \tag{29}$$

$$\delta f_{i+1/2} = F_{i+1/2} - f_{i+1/2}. \tag{30}$$

The quantities ρ_i^* represent a first-order update in which monotonicity has been preserved. The second-order scheme above does not preserve monotonicity so we must filter the flux-corrections by using a local algorithm called a flux-limiter. This filter, which forbids the enhancement of extrema, is the heart of the FCT technique. The simplest form is the one originally proposed by Boris and Book [1]:

$$\begin{aligned}\delta f_{i+1/2} \to \operatorname{Sgn}(\delta f_{i+1/2}) \max\{0, \min[|\delta f_{i+1/2}|, \\ \operatorname{Sgn}(\delta f_{i+1/2})(\rho_{i+2}^* - \rho_{i+1}^*), \operatorname{Sgn}(\delta f_{i+1/2})(\rho_i^* - \rho_{i-1}^*)]\}\end{aligned} \tag{31}$$

where

$$\operatorname{Sgn}(x) = \begin{cases} 1, & x \geqslant 0 \\ -1, & x < 0. \end{cases} \tag{32}$$

Generalizations of the above, including extension to multidimensional systems without timestep splitting, have been given by Zalesak [10]. The hybrid scheme is now completed as follows:

$$\rho_i^{n+1} = \rho_i^* - \delta f_{i+1/2} + \delta f_{i+1/2}. \tag{33}$$

In summary, ρ^n, u^n, and ϕ^n are taken to be known and ρ^{n+1} is obtained by execution of the following steps in order: Eqs. (8), (7), (21), (24), (27), (21) with F for f, and (29)–(33).

3. Numerical Experiments

Let us consider an inviscid Burger's equation cast in a moving frame of reference

$$\rho_t + \left(\frac{a}{2}\rho^2 - v_0\rho\right)_x = 0 \tag{34}$$

where a and v_0 are constants. The v_0 term is added to demonstrate the robustness of the method against expansion shocks. Let the initial condition be

$$\rho_0(x) = \max(0, bx(x_0 - x)); \qquad x \geqslant 0 \tag{35}$$

$$\rho_0(-x) = -\rho_0(x). \tag{36}$$

The result is a pair of antisymmetric parabolic lobes shown in Fig. 3a. Within each lobe an analytic solution can be found from Eq. (5).

The second benchmark for the method is a square wave initial density profile of unit amplitude which is advected with constant velocity v_0. The solution is

$$\rho = \begin{cases} 1, & 0 < x + v_0 t < x_0 \\ 0, & \text{otherwise.} \end{cases} \tag{37}$$

This test is of value in determining the degree of numerical diffusion and dispersion in an algorithm.

Before applying the new method to the solution of these test problems, we want to give examples of the pathologies to which we alluded in the Introduction. If one uses a common FCT method (with a spatially centered second-order correction) on the evolution of the parabolic lobes just considered, staircases will form as shown in Fig. 1. This pathology is not a result of nonlinear wave propagation, but is connected with the shape of the profile. The same behavior is seen when a semicircular profile is transported by linear advection. Because the slope of the function changes continuously from a finite toward an infinite value, there is some point on the curve for which the centered finite-difference derivative begins to produce Gibbs oscillations. When these are clipped by the flux limiter, the staircases appear. Other investigators have found that when this pathology occurs, it can be remedied by adding an explicit viscous dissipation term to the high-order correction [12]. The totally upwind scheme, as we shall demonstrate, is free of these staircase structures without modification. This is because the high-order upwind scheme does not produce

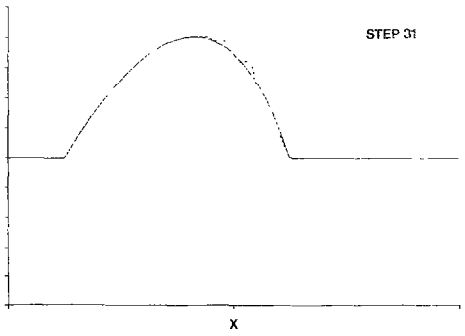

FIG. 1. Nonlinear evolution of a parabolic pulse lobe using a common FCT algorithm with centered differences. The figure shows the development of nonphysical staircase structures on the forward slope. The solid line is the analytic solution. The dashed line is the numerical result.

an unphysical backward propagation of dispersive ripples resulting from an impulsive change in slope.

An example of another pathology motivating our approach is pictured in Fig. 2. Early attempts to simulate a drifting N-wave shock using the flow velocity as a switching criterion resulted in loss of accuracy at flow reversals in the region of expansion. In the example, a sizable "glitch" occurs near the place where the flow speed reverses sign. This does not occur when the characteristic speed is used to determine the upwind direction.

The first test of the new method is the development of an N-wave shock from the antisymmetric parabolic lobe profile of Eqs. (35) and (36). In (34), v_0 is taken to be zero.

Defining the flux at each grid point by

$$\phi_i = \frac{a}{2}\rho_i^2 \tag{38}$$

we apply the upwind-FCT hybrid on a grid of 202 points with periodic boundary conditions. For comparison, each run is repeated without the second-order correction. The test is completely specified by setting the maximum Courant number and the number of grid points per lobe: $|u|_{\max}\,\delta t/\delta x = 1/4$; $\delta x = x_0/40$. For these parameters, the shock is expected to form at step 41. Figure 3 shows the initial condition and results of the first-order and hybrid schemes. Note that after step 41 (when the shock is expected to form) the hybrid scheme demonstrates increasingly better performance, both in the location of the shock and in the sharpness of the profile.

Our second experiment is like the first, but with the addition of a constant drift v_0; i.e., we define the flux at the grid points by

$$\phi_i = \frac{a}{2}\rho_i^2 - v_0\rho_i. \tag{39}$$

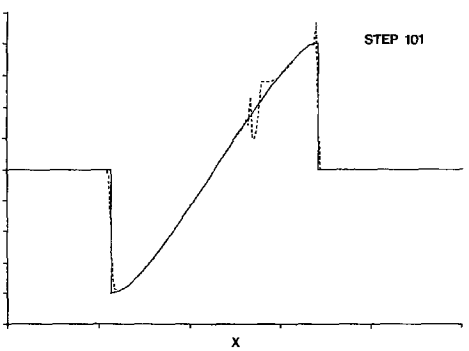

FIG. 2. The development of non-physical expansion shocks in the numerical solution (dashed lines) occurs when the flow speed direction is used instead of the characteristic speed direction in the upwind switching.

The value of v_0 is chosen such that the characteristic speed reverses sign where ρ is equal to 0.35 of its maximum. The timestep is the same as for the previous case, but because of the added drift the Courant number is raised to 0.3375. In this example, the distinction between the characteristic speed $u = a\rho - v_0$, and the local flow speed $v = \frac{1}{2}a\rho - v_0$ becomes important. Tests of the scheme using v instead of u in deter-

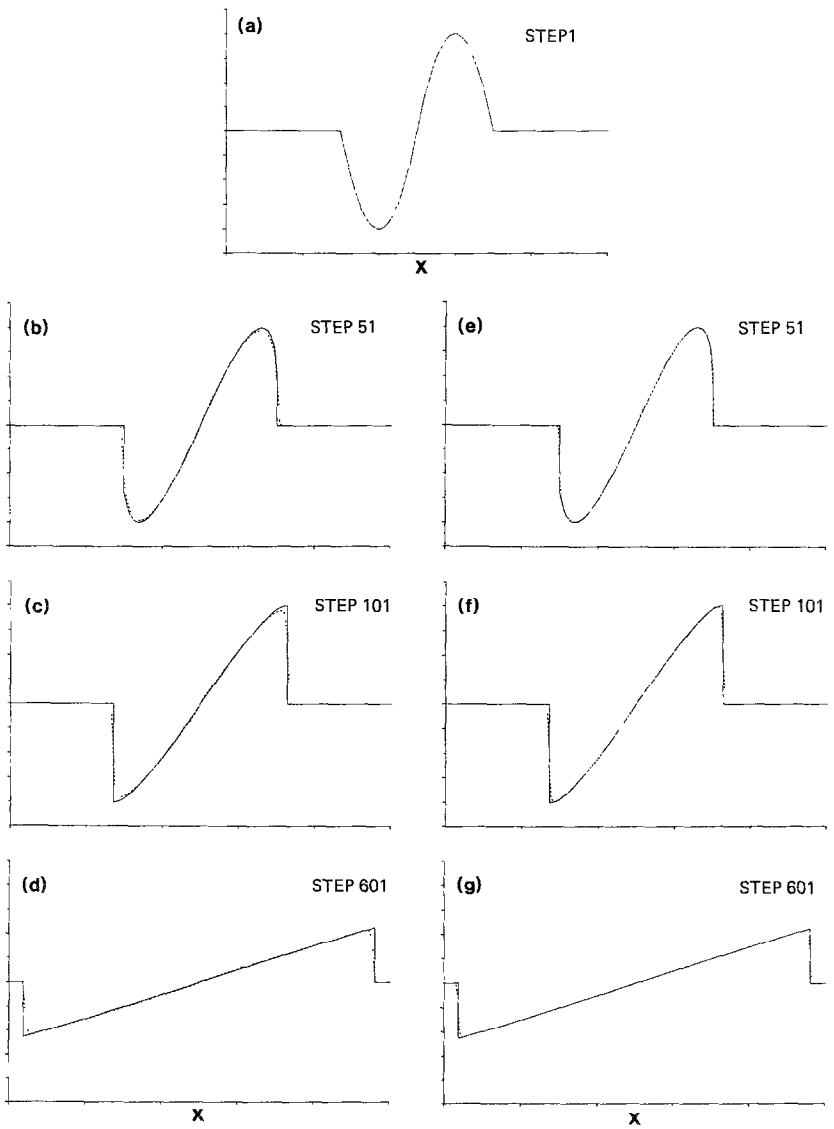

FIG. 3. Symmetric N-wave shock development. Solid line: analytic solution; dashed line: numerical solution. First-order results are given in b–d; second-order in e–g.

mining the upwind direction invariably caused the growth of spurious expansion shocks as shown in Fig. 2.

Figure 4 illustrates the results for our second test. A comparison with Fig. 3 reveals increased dissipation in the first-order scheme as a result of the increased Courant number. However, the second-order results are much less sensitive and still show good agreement with the analytical results.

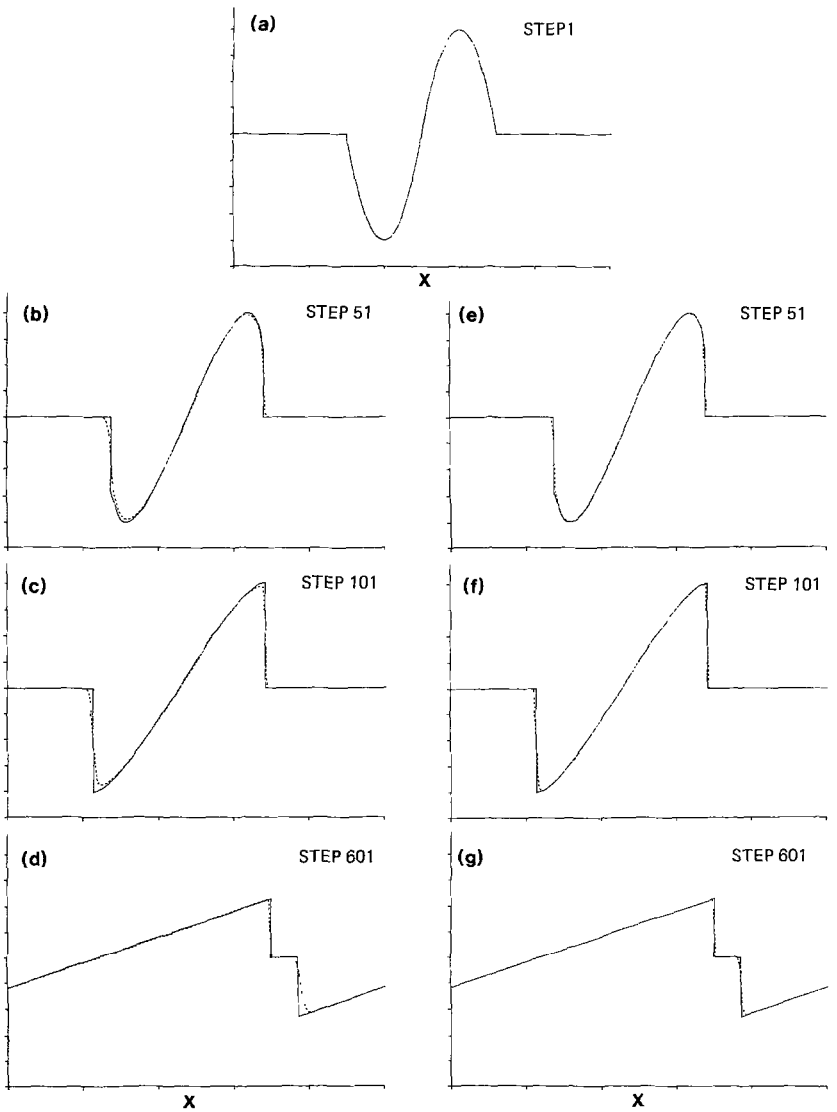

FIG. 4. Drifting N-wave demonstrating stability against expansion shocks (see Fig. 2). The characteristic speed vanishes where the amplitude is 35 percent of initial maximum. For legend see Fig. 3. The step-like structure at step 601 is a result of periodic boundary conditions.

The final experiment is the square-wave test problem. In this test the profile of (37) is convected leftward with a constant velocity giving a Courant number of 0.25. The flux at the grid points for this case is simply $\phi_i = -v_0\rho_i$. The results Figs. (5e)–(g) preserve the sharpness of the square wave to a reasonable degree after advection through 150 cells (step 601). The first-order results Figs. (5b)–(d), however, show complete loss of sharpness by this point.

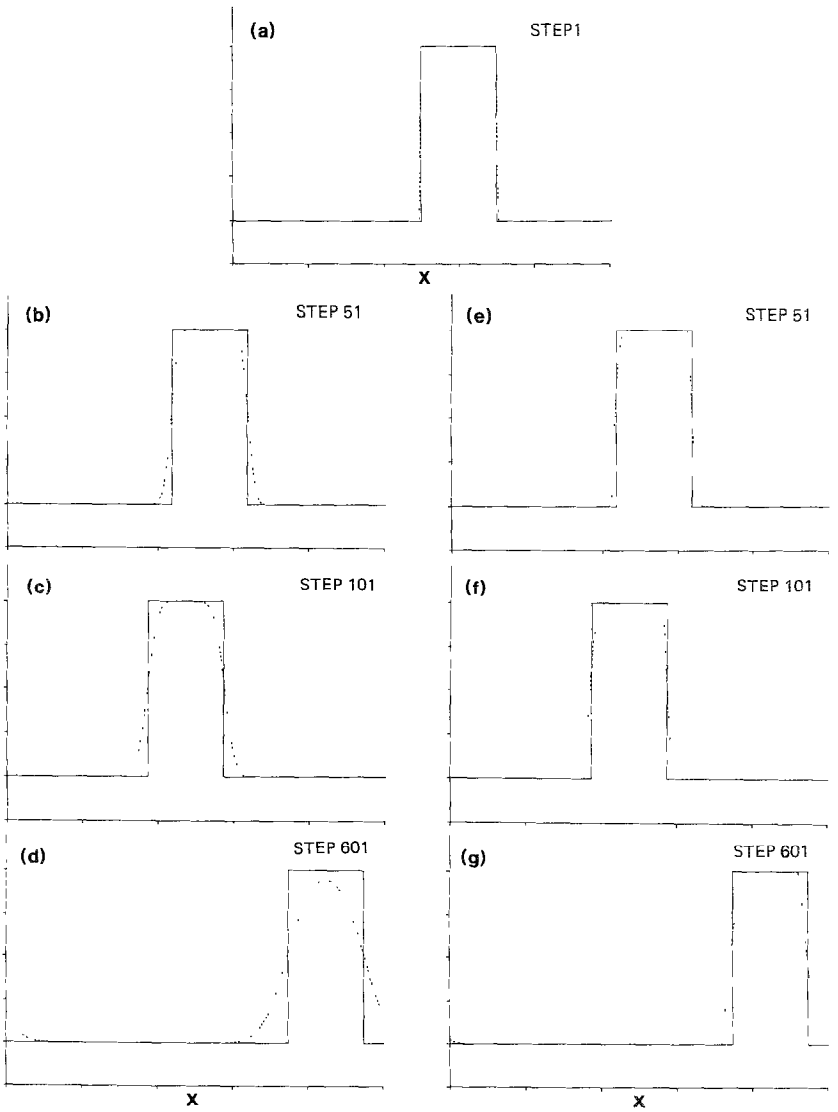

FIG. 5. Linear advection of a square wave. Solid line: exact solution; dashed line: numerical solution. First-order results appear in b–d; second in e–g.

4. Summary and Conclusion

High-order upwind differencing, properly filtered for monotonicity preservation, yields a substantial improvement over comparably filtered central differencing when applied to scalar hyperbolic systems describing shock formation. In our work, this filtering consists of flux correction to a first-order upwind scheme. The first-order scheme takes for the upwind direction the direction of a numerically defined characteristic speed, as opposed to the actual flow speed. Monotonicity is preserved in each of four possible combinations of upwind directions on either side of a grid point. Directional information from the first-order scheme is also used to obtain the second-order corrections to the fluxes. Expansion shocks are precluded by a one-point flux adjustment. Our second-order method extends in a strightforward way to higher-order differences. It also gives accurate shock propagation speeds as a result of being cast in flux conservative form. That the method achieves the proper development of shocks from smooth data has been confirmed by comparison with analytic solutions. We attribute the success of the method to the sampling of data exclusively from the direction from which the information arrives (i.e., the relevant characteristic direction).

Acknowledgment

This work was supported by the Office of Naval Research.

References

1. J. P. Boris and D. L. Book, *J. Comput. Phys.* **11** (1973), 38.
2. S. K. Godunov, *Math. Sb.* **47** (1959), 271; also, Cornell Aero. Lab. Transl.
3. A. Harten, *Commun. Pure Appl. Math.* **30** (1977), 611.
4. A. Harten, P. D. Lax, and B. van Leer, *SIAM Rev.* **25** (1983), 35.
5. A. Harten, *J. Comput. Phys.* **49** (1983), 357.
6. B. van Leer, "On the Relation between the Upwind-Differencing Schemes of Godunov, Enquist–Osher, and Roe," ICASE Report 81–11, NASA Langley Research Center, 1981.
7. B. van Leer, *J. Comput. Phys.* **23** (1977), 276.
8. P. J. Roache, "Computational Fluid Dynamics," p. 67, Hermosa, Albuquerque, New Mexico, 1982.
9. R. F. Warming and R. M. Beam, *AIAA J.* **14** (1976), 1241.
10. S. T. Zalesak, *J. Comput. Phys.* **31** (1979), 335.
11. S. T. Zalesak, *in* "Proceedings, Fourth IMACS International Symposium on Computer Methods for Partial Differential Equations, Lehigh Univ., 1981."
12. S. T. Zalesak, private communication.